Alteration of Protein Constituents Induced by Low-Energy (<40 eV) Electrons. III. The Aliphatic Amino Acids

H. Abdoul-Carime and L. Sanche*

Groupe des Instituts de Recherche en Santé du Canada, Faculté de Médecine, Université de Sherbrooke, Sherbrooke, Québec J1H 5N4, Canada

Received: March 31, 2003; In Final Form: October 23, 2003

We report mass spectrometric measurements of anions desorbed by 1−40 eV electron impact on thin films of glycine (Gly), alanine (Ala) and cysteine (Cys) physisorbed on a Pt substrate. (H^-, CH^-, CH_2^-, CH_3^-, O^-, OH^-, and CN^-), (H^-, CH_2^-, CH_3^-, O^-, and OH^-), and (H^-, O^-, OH^-, and CN^-, S^-, and SH^-) anions are observed to desorb from these irradiated molecular solids, respectively. The anion yield functions exhibit structures at energies below 15 eV, indicating that molecular dissociation operates via dissociative electron attachment (DEA). Above 15 eV, anion desorption is dominated principally by nonresonant dipolar dissociation (DD). However, an additional structure observed at 20 eV in the yield function of H^- denotes the presence of a resonant process: DEA or decay of a transient molecular anion into the DD continuum or both. The presence of the sulfur group in cysteine enhances dissociation by 2 orders of magnitude relative to Gly and Ala.

I. Introduction

The action of ionizing radiation on biological cells is strongly implicated in health and various human activities (e.g., medical diagnosis and treatment, food treatment, travel).[1−5] It is now well admitted that high-energy particles cannot only induce genomic diseases (e.g., cancer, mutations) but, paradoxically, can also provide an efficient tool to treat tumors.[1] In the food industry, ionizing radiation is applied to guarantee quality and preservation against food-born bacteria and parasitic organisms.[2−4] Aircrew and astronauts are also subject to ionizing particles (such as high-energy cosmic rays and solar particles).[5] Thus, to improve radiation protection and radiation technology in these fields, it is necessary to understand in a greater detail the action of high-energy radiation penetrating biological organisms. Furthermore, the knowledge gained from basic experiments may have the potential to better predict and control the effects of ionizing radiation.

At short time scales (less than a femtosecond), the penetration of high-energy particles within biological tissues generates along their ionization tracks various reactive species, such as neutral and ionic radicals, as well as a large number of *secondary low-energy electrons* ($\sim 4 \times 10^4$/MeV).[6−8] Once produced within biological systems, these radiation-induced products are able to react with cellular constituents (nucleic acids, proteins, peptides, etc.) and to cause irreversible damage. For instance, free radicals are well-known to alter DNA[9,10] and modify the structure of proteins.[11,12] Although less investigated until very recently, low-energy (<40 eV) electrons (LEEs) have also been shown to induce damage to nucleic acids, in terms of single, double, and multiple double-strand breaks.[13,14] The degradation is initiated at the molecular level[15] by the fragmentation of the nucleic acid building blocks, that is, DNA bases, backbone sugar, and structural water.[16−18] Therefore, these LEEs are also likely to damage peptides and proteins in a similar manner, by altering their constituents and some specific bonds.[19]

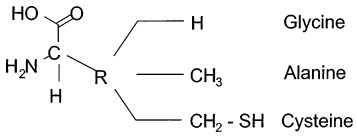

Figure 1. Structure of glycine, alanine, and cysteine. NH_2−CHR−COOH is the common atomic composition for all three amino acids; R represents H, CH_3, and CH_2−SH, respectively.

The present report is the third of a series intended to investigate the damage to condensed protein constituents induced by LEEs.[19,20] The previous research was dedicated to the investigation of the action of LEEs on disulfide or acetamide bonds[19] or both and some selected amino acids containing cyclic groups.[20] Here, we investigate LEE-induced fragmentation of the some selected aliphatic amino acids condensed on a platinum substrate, namely, glycine (Gly), alanine (Ala), and cysteine (Cys). These amino acids have the simplest structures (Figure 1) found among the different amino acids that constitute protein and peptide building blocks. Glycine presents the fundamental pattern structure for most amino acids (Figure 1). The next slightly more complex structure is alanine, for which the methyl, CH_3, group replaces the hydrogen atom located at the carbon site. Substitution of the methyl (CH_3) group of Ala by the CH_2−SH group transforms alanine to cysteine.

II. Experiment

The apparatus used in the present investigation has been described in detail elsewhere.[18,21] Only a brief description of the procedure and experimental arrangement is given here. The condensed films of amino acids are made from evaporation of the powder (Aldrich Ltd.). Approximately 50 mg is placed in a miniature oven located within a load-lock chamber. In this chamber, the compounds are further purified by continuously

* Corresponding author. Léon Sanche, Dép. Médecine Nucléaire et Radiobiologie, Faculté de Médecine, Université de Sherbrooke, Sherbrooke, Québec J1H 5N4, Canada. Tél.: (819) 346-1110, ext. 14907. Fax: (819) 564-5442. E-mail: Leon.Sanche@USherbrooke.ca. Canada Research Chair in the Radiation Sciences.

10.1021/jp030413x CCC: $27.50
Published on Web 12/10/2003

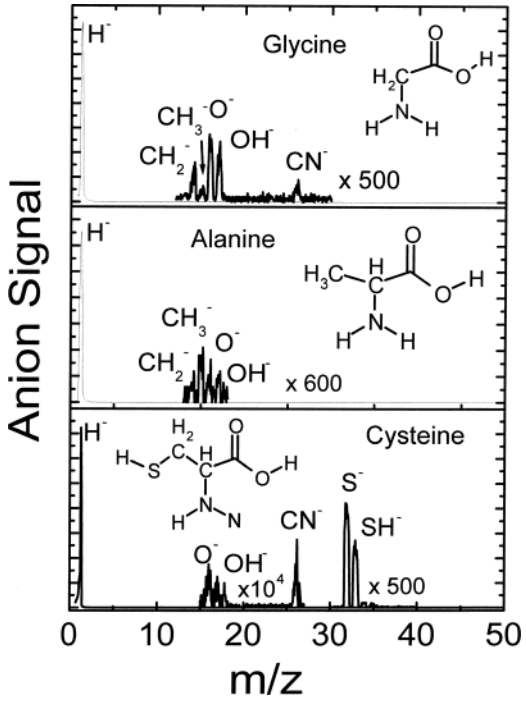

Figure 2. Mass spectrum and structure of (a) glycine, (b) alanine, and (c) cysteine. The mass spectra are obtained by bombarding a 10 monolayer (ML) thick film with a 400 nA beam of 28 eV electrons.

heating and pumping. Afterward, the oven is transferred into the measurement chamber via the gate valve and positioned at approximately 1 cm in front of a 2 cm^2 platinum (Pt) foil. The latter is cleaned prior to each deposition by resistive heating to ~1000 °C for about 10 s. After repeated heating cycles, the surface of the platinum foil forms azimuthally disordered Pt-(111) domains.[22] The aliphatic amino acids are thermally evaporated onto the Pt surface held at room temperature. This film-growth technique produces samples with purity higher than 99%.[23] [Levesque, P. L.; Michaud, M.; Sanche, L., manuscipt in preparation.] The evaporation temperatures for deposition of Gly, Ala and Cys are 110, 118, and 100 °C, respectively. These temperatures usually correspond to approximately the threshold for detection of the compound by analyzing the residual gas. At such relatively low temperatures, these amino acids are likely to be evaporated without being chemically degraded. In fact, it has been reported that evaporation of tryptophan powder at a temperature of 150 °C, that is, approximately 100 °C lower than the typical decomposition temperature, T_{dec}, does not deteriorate the structure of the molecule.[23,24] Since here the operating temperatures are at least 100 °C below the typical amino acid decomposition temperatures (e.g., T_{dec} of glycine is 200 °C), the vaporized molecules are also not likely to be denatured.

The condensed film is oriented toward the entrance of a mass spectrometer (Extrell 150-QC), which is equipped with an ion lens to increase the collection efficiency of the detection system. The electron beam with an energy spread of 0.5 eV full width at half-maximum (fwhm), produced by a commercial electron gun (Kimball Physics Inc. ELG-2), impinges on the film at an incident angle of 70° from the surface normal for no more than 60 s with a current that can be varied from 5 to 500 nA. The incident electron energy is calibrated by monitoring the onset of the current transmitted through the film.[25] With this apparatus, we can measure (1) the relative magnitude of the desorbed anion signals as a function of the *m*/*e* ratio at a fixed incident electron energy (i.e., Figure 2) and (2) the magnitude of the detected yield of a single anion as a function of the incident electron

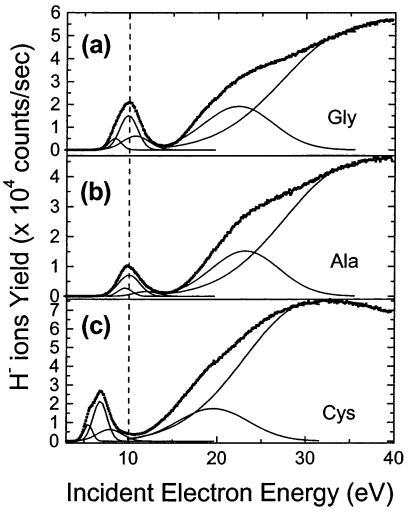

Figure 3. Energy dependence of the H^- ion yields desorbed by electron impact on a 5 ML (a) glycine, (b) alanine, and (c) cysteine film. The smooth solid curves are individual Gaussian functions fitted to the data.

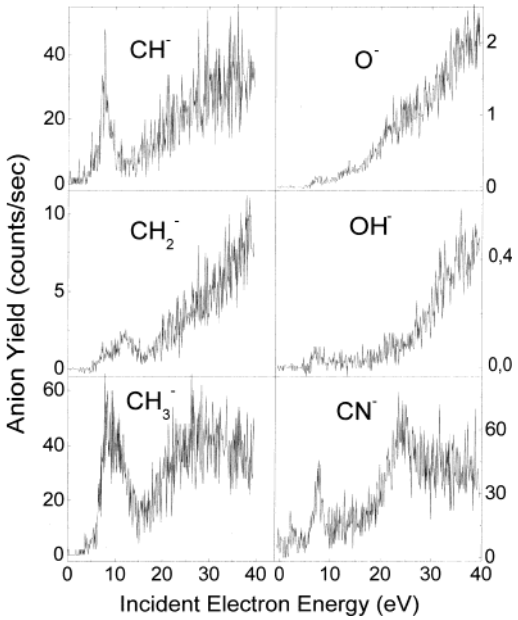

Figure 4. Electron energy dependence of the (a) CH^-, (b) CH_2^-, (c) CH_3^-, (d) O^-, (e) OH^-, and (f) CN^- ion yields desorbed from 200 nA low-energy electron bombardment of about 10 ML physisorbed films of glycine.

energy, that is, the anion yield function (Figures 3−6). The number of anions measured at the detector of the mass spectrometer does not represent the absolute amount produced. Due to the limited number of anions that escape the surface and the low efficiency of anion detection, the reported yields may be orders of magnitude smaller than actual values. In our system, the anion detection efficiency (e.g., ion collection, transmission into the quadrupole) is approximately identical for the "heavy" anions, that is, those above 10 amu. Thus, we can then compare for films of the same thickness the relative intensity of high-mass negative species in terms of the fraction of a negative fragment produced per incident electron. Such a comparison is not possible with lighter anions, since in this lower mass regime the transmission of our mass spectrometer can change significantly as a function of *m*/*e*, particularly for H^-.

The film thickness is determined within 50% accuracy by correlating evaporation times to saturation of the anion signals:[21,26] typically, the curve of the anion signal vs evaporation time

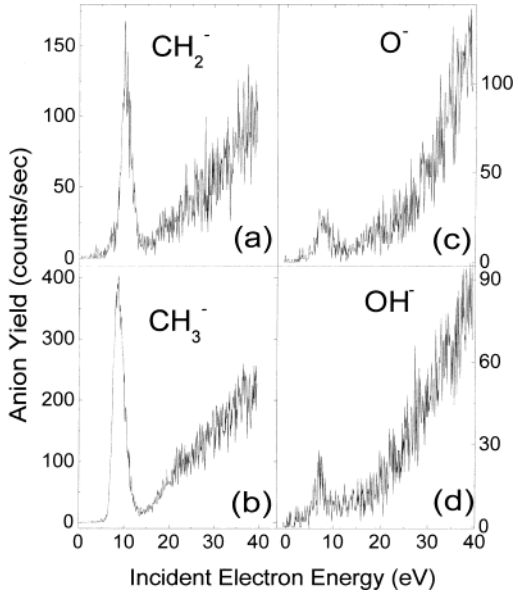

Figure 5. Incident electron energy dependence of (a) CH_2^-, (b) CH_3^-, (c) O^-, and (d) OH^- ion yield desorbed under 400 nA electron bombardment of an approximately 10 ML thick film of alanine.

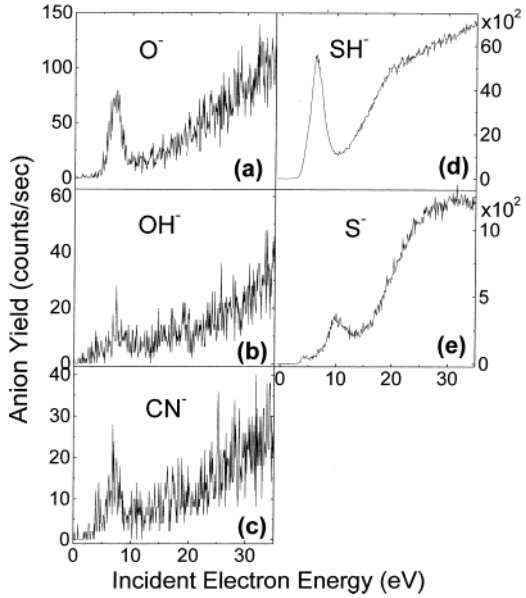

Figure 6. Incident electron energy dependence of (a) O^-, (b) OH^-, (c) CN^-, (d) S^-, and (e) SH^- ion yield desorbed under 400 nA electron bombardment of about 10 ML thick film of cysteine.

exhibits an increase that reaches a plateau at a film thickness of approximately 5 monolayers (ML). In the present work, mass spectra were recorded with a thickness of 10 ML and anion yield functions with a thickness of 5−10 ML. At these thicknesses, anion electron stimulated desorption (ESD) arises principally from the first few layers near the film−vacuum interface with little or no signal emanating from molecules, which may have been modified by contact with the Pt substrate. It has been reported that Gly deprotonates upon adsorption onto a Cu(110) surface[27] or decomposes to CO_2 and CH_3NH_2 on a metal and oxide surface.[28] These results indicate that dissociative chemisorption of Gly may also occur on our platinum substrate and thus justifies the use of films no thinner than 5 ML.

III. Results

Figure 2 exhibits mass spectra obtained from a 28 eV, 0.4 μA incident electron beam impinging onto 10 ML films of (a) glycine, (b) alanine, and (c) cysteine. As seen from the mass spectra, H^- is the predominant anion. We also observe other negative fragments of lower intensity, such as (a) CH^-, CH_2^-, CH_3^-, O^-, OH^-, and CN^-, (b) CH_2^-, CH_3^-, O^-, and OH^-, and (c) O^-, OH^-, CN^-, S^-, and SH^-. According to the natural abundance of ^{34}S relative to that of ^{32}S (referred to as S in the text),[29] the peaks appearing on right of the SH^- peak in the mass spectrum of cysteine in Figure 2 are due to $^{34}S^-$ and $^{34}SH^-$ desorption. From further consideration of the isotopic ratios, the $^{33}S^-$ species is expected to make only a small contribution to the 33 amu signal. Thus, the 33 amu peak is mainly attributed to desorbing SH^- ions. No negative fragments heavier than $^{34}SH^-$ are detected to desorb from our irradiated films. If formed, such species may not possess sufficient kinetic energy to overcome the attractive forces (image−charge, polarization, etc.) induced by the dissociating anion in the film and substrate.[30] Huels and collaborators have observed from low-energy electron impact on gaseous glycine the production of larger mass anions, for example, $(Gly\text{-}H)^-$, $COOH^-$, and $H_2NC_2O^-$,[31] which are not detected here. Thus, these species could be produced and remain trapped in our films.

The 16 amu negative fragment seen in Figure 2 raises particular attention. It can be attributed, a priori, to O^- or NH_2^-, since our mass spectrometer cannot resolve the fine structure at this mass. However, in several previous experiments on electron impact on molecules containing amino groups, no production of NH_2^- anions were reported.[32−34] Moreover, the larger positive electron affinity of O (1.46 eV) compared to that of NH_2 (0.78 eV)[35] may favor the formation of the oxygen anion. We therefore *tentatively* attribute the nature of the 16 amu peak anion to O^-.

Similarly, the 15 amu negative fragment can be a priori attributed to CH_3^- or NH^- or both, which have similar electron affinities (0.1 and 0.4 eV, respectively).[35] However, from the fact that NH^- is produced from NH_2, we expect to detect this anion not only from glycine, alanine and cysteine but also from tryptophan, histidine, and proline.[20] For instance, the 16 amu has been observed for all of the mentioned substances. We did not detect 15 amu fragments for Cys, Trp, His, and Pro. Therefore, NH^- is not expected to be produced, although we cannot completely rule out this possibility.

Figures 3−6 represent the negative fragment yield functions (Table 1 lists the peak positions in the yield functions). Peaks or maxima are clearly visible in most of these curves. Above ~12 eV, a continuously rising signal is recorded on which, in most of the curves, peaks are superimposed. The yield functions of H^- in Figure 3 were obtained from irradiation of 5 ML thick films of (a) glycine, (b) alanine, and (c) cysteine by a 6 nA electron beam. Heavier negative anion yield functions were recorded from exposure of 10 ML amino acid films to a 200 nA (Figure 4, glycine) and a 400 nA (Figures 5 and 6, alanine and cysteine, respectively) electron beam. In each case, the 1−40 eV range is scanned within 20 s; each film is scanned five times, and the curves are compared to ensure that they are all identical. Although relatively high currents are required to produce the detectable higher mass anions, charging of the irradiated solids has not been observed from these comparisons. If it had occurred, a shift of peaks in the anion yield functions or the electron transmission function to the substrate or both toward higher energies would have appeared with increasing irradiation times.

The H^- anion yield function measured from electron bombardment of glycine films (Figure 3a) is similar to that recorded from alanine films (Figure 3b). Both experimental curves present

TABLE 1: Positions of Peaks (eV, ±0.5 eV) in the Anion Yields Produced from 1−40 eV Electron Bombardment of Thin Film of Glycine (Gly), Alanine (Ala), and Cysteine (Cys)[a]

	H^-	CH^-	CH_2^-	CH_3^-	O^-	OH^-	CN^-	S^-	SH^-
Gly							2.5[a]		
			4.9[a]	4.5[a]					
	8.4	7.1	7.4	7.5	7.5	7.5	7.5		
	9.8								
	10.7			10.4					
			11.7						
	20.6								
Ala			7.1		7.6	7.6			
				8.3	8.5				
	9.6			9.6					
	10.1		10.2						
	11.9								
	23.0								
Cys							4.1	4.6	
	5.6								6.2
	6.9				7.2	7.2	7.2		7.0
	8.2								
								10.0	10.2
	19.7								
								22.0	22.0

[a] Shoulder or a faint peak.

a broad structure at around 10 eV and an additional structure at around 22−23 eV. The broad 10-eV structure in the energy dependence of the H^- yield from glycine and alanine can be represented as a convolution of three Gaussian functions of approximately 3−5 eV full width at high-maximum centered at (8.4, 9.8, and 10.7 eV) and (9.6, 10.1, and 11.9 eV), respectively. In contrast, the H^- deconvoluted peaks from dissociation of cysteine are downshifted in energies at 5.6, 6.9, and 8.2 eV. The fitted Gaussian functions are shown by the solid lines in Figure 3. Above 10 eV, the broader Gaussian functions are centered at approximatively 23, 23, and 20 eV for anion desorption from Gly, Ala, and Cys, respectively.

IV. Discussion

Among all biological molecules, the structure of amino acids is certainly the one that presents a peculiar characteristic. In isolation (i.e., gas phase or matrix), amino acids exhibit a stable non-charge-separated structure,[36−39] which is represented here by $NH_2-CHR-COOH$ (R = H, CH_3, and CH_2SH for Gly, Ala, and Cys, respectively), as shown in Figure 1. However in the solid state, amino acids may adopt a zwitterionic arrangement.[40−44] The zwitterion structure is obtained by transferring a proton from the carboxylic acid (COOH) group toward the amino (NH_2) group, leaving the molecule in the $NH_3^+-CHR-COO^-$ conformation. Conversion from neutral to the "twin-ionic" structure has been recently observed from photoelectron spectroscopy experiments[45] and studied theoretically.[46] Bowen and co-workers have reported that glycine requires at minimum five hydration waters to induce the zwitterion form; phenylalanine and tryptophan need four.[45] Therefore here, since LEEs impinge on approximately 5 ML thick films, they are likely to interact with the zwitterionic configuration. Even though many LEE-impact experiments have been performed on non-charge-separated neutral molecules,[47−49] information on zwitterions is still scarce, to date.[23]

Most of the desorbed anion yield functions shown in Figures 3−6 exhibit pronounced maxima superimposed on an increasing monotonic background. This behavior can generally be attributed[15,17−19,50−54] to a contribution from the formation of dissociative transient molecular anions (TMA), which produce the peaks, and another contribution from dipolar dissociation (DD). Whereas in gaseous molecules stable anion yields are usually produced with much more intensity by DEA than by DD,[47] the relative yields are observed to be much different in electron stimulated desorption from molecular solid surfaces.[15,17−19,50−54] As explained by Sambe et al.,[30] the extra energy provided by the polarization of the medium by the remaining positive charge during DD propels the anion in a vacuum with much more kinetic energy than in the case of DEA; this changes the relative intensities between DD and DEA. At incident electron energies above ∼5 eV, formation of a TMA prior to fragmentation is likely to arise from a core-excited resonance consisting of two electrons trapped in excited orbitals by a core hole, that is, a one-hole two-electron state.[54,55] Since a dissociative anion state occurs at a specific resonance energy, corresponding to a given orbital configuration, it produces an energy-localized maximum or peak in the anion yield function as shown in Figures 3−6. The width of the peak arises from a convolution of the dissociation and resonance widths, which is broadened by extrinsic effects[52] such as multiple electron scattering in the film prior to attachment. The resonance width depends on the lifetime of the resonance, and the dissociation width represents the energy window accessible in the Franck−Condon region for electron attachment from the ground state configuration to form the dissociative anion. Consequently, DEA is strongly dependent upon the orbital configurations of the target molecule.

In the case of amino acids, molecular orbitals may differ, depending whether the molecule is in its "neutral" or zwitterion form.[27,44,56,57] For instance, it has been found that the highest occupied molecular orbital, HOMO, of the nonionic form of glycine is the N 2p lone pair orbital, corresponding to the $3a_1$ orbital of the free ammonia. On the other hand, for zwitterionic glycine, the removal of the proton from the carboxylic functional (−COOH) group gives rise to an essentially oxygen lone pair HOMO.[27] Additionally the proton transfer to the amino group produces a very large dipole moment[44,56] on the amino acid that could substantially stabilize the lowest unoccupied molecular orbital, giving rise to a bound valence anion state of the zwitterion.[57,58] Therefore, in gas-phase experiments the position of resonant structures observed in the yield functions of anion fragments induced by LEEs or in electron scattering cross sections[31,57] may differ from those detected in the condensed phase.

In the case of DD, anion production results from the dissociation of a neutral excited state into a positive and a negative ion; this latter can be detected in anion yield functions.[19,52,53] Unless transient anions decay in the DD channel, the anion signal arising from DD does not exhibit any structure, since it is governed by direct (nonresonant) electronic excitation via inelastic scattering of the incoming electron. The dissociation limits for ion pair formation usually lie at much higher energies than the neutral ground-state dissociation limit. Thus vertical transitions to excited states leading to ion pairs are usually not observed below the first ionization limit.[17−19,21,25,26,32] However, since in the zwitterion configuration the charges are already separated, the lowest dissociation limit for opposite charge fragments is expected to lie at a lower energy (with respect to the ground state) than in the neutral configuration. Thus, for zwitterions DD may occur at lower energies. Finally, we note that below the DD threshold, DEA is the only mechanism that leads to anion fragments.[19,52,53]

Desorption of H^- from Films of Glycine, Alanine, and Cysteine. The structure below 12 eV in Figure 3 indicates the formation of core-excited TMA and their decay into the DEA channel. Moreover, for the structures observed at 9.8 and 10.7 eV for the glycine films (Figure 3a) and those at 9.6, 10.1, and 11.9 eV for the alanine films (Figure 3b), the core-excited resonances may be formed of two electrons in Rydberg excited states of the molecule bound to the positive ion core (i.e., the grandparent model) and dissociate via curve crossing with a dissociative valence state.[54,55] Indeed, for various molecules, it has been observed that such Rydberg anionic states lie typically 4 eV below their corresponding positive ions.[54,55] Therefore, measurements of ionization potentials of glycine at 13.6, 14.4, 15.0, and 15.6 eV[59] support such an assignment for the peaks observed in the H^- yield function of glycine. The overall symmetry of these excited orbitals is of the s-type, so electronic excitations should involve predominantly σ orbitals.[59] The molecular structure of Ala is closely similar to that of Gly but differs only by the absence of the methyl group on glycine. Thus, any similarity within the H^- yield functions reported here for both amino acids suggests that anion dissociation is localized on the same group. The 9.6 and the 10.1 eV ($\pm$0.5 eV) resonances therefore possibly arise from the capture of the extra electron on the twin ion (i.e., $NH_3^+-...-COO^-$) group.

More surprisingly, the energy dependence of H^- anions desorbed from electron irradiation of films of cysteine differs from those obtained from Gly and Ala films. Since the three molecules have a common zwitterionic group, some structures around 9−12 eV are expected to be seen. Instead, four peaks appear at 5.6, 6.9, 8.2, and 19.6 eV (Figure 3c) in the H^- yield function of cysteine. They most likely arise from core-excited resonances formed by an incoming electron trapped by positive electron affinity of excited states (e.g., π^* or σ^* or both) of the target molecule. If the potential energy curve of the transient cysteine anion, $(NH_3^+-HCCH_2SH-COO^-)^{*-}$, is dissociative along any coordinate leading to ground state H^-, unimolecular dissociation can take place and H^- and its neutral counterpart are produced. As the twin-ion group is the common feature to all three investigated amino acids, the fact that we do not observe clearly resonance structure common to Ala and Gly (i.e., peaks located at approximately 9.6 and 10.5 eV) in the H^- yield function of cysteine suggests that this anion is not likely to be produced from the dissociation of the $NH_3^+-...-COO^-$ group. Therefore, it may arise predominantly from the dissociation of CH_2-SH end of Cys.

Finally, an additional structure is observed in the H^- yield function of Gly and Ala at around 23 eV. The origin of this peak is more difficult to interpret, since it lies well within the DD energy range, where resonance features may arise from either DEA or decay of the transitory anion into the DD continuum. For the latter mechanism, which has been recently observed to occur in molecular solids,[18,60] the TMA at 23 eV must decay into an electronically exited state by ejecting the excess electron. The excited state then undergoes unimolecular dissociation into H^- and its corresponding radical cation. DEA may also occur via the dissociation of a TMA centered near 23 eV or the fragmentation of an anion located at lower energy if, prior to attachment, the electron suffers a large energy loss via electronic excitation of a molecule. For instance, a 23 eV incoming electron could lose an energy of 12 eV by exciting an electronic state, thus lowering its energy to approximately 11 eV, at which energy it could reproduce the 11 eV DEA process. Such double events, however, would necessarily lead to an intensity of the H^- ion yield at 23 eV weaker than that at 11 eV. It has been shown that the signal of negative ions generated via double or multiple events is significantly weaker (i.e., typically 1 order of magnitude) than those formed under single attachment conditions at lower energy.[61] The yield function of H^- (Figure 3) shows that the energy-integrated magnitude of the peak located at 23 eV is larger than that located at 11 eV. Hence, a considerable portion of the H^- signal at 23 eV must arise from resonant DD or a TMA located near 23 eV or both, although some small multiple event contributions could be present.

Production of Heavier Anions from Films of Glycine, Alanine, and Cysteine. A resonance peak located at around 7.5 ($\pm$0.5) eV is observed in the yield functions of the O^-, OH^-, and CN^- anions produced from LEE (<40 eV) impact onto glycine and cysteine films (Figures 4 and 6). From irradiation of alanine films with the same incident electron energy, only O^- and OH^- anion fragments have been detected (Figure 5c,d); CN^- fragments are not seen. This observation does not necessarily imply that no CN^- is produced during electron impact on Ala solids but that the signal lies below the detection limit. The fact that the yield functions of O^-, OH^-, and CN^- anions present the same resonance peak at 7.5 eV is indicative that, at this energy, the extra electron is captured and localized on the twin ion, $NH_3^+-...-COO^-$ group of the molecule.

The first ionization potential of glycine is 13.6 eV;[59] thus, the resonance energy should lie around 9.6 eV[57] if the TMA involved a Rydberg transition. The anion peaks located at 7.5 eV in Figures 4, 5, and 6 are therefore not likely to arise from Rydberg core-excited resonances but probably involve two electrons in valence excited orbitals. The anions O^-, OH^-, and CN^- have also been reported from DEA to gaseous glycine at approximately 6 eV.[31] The shift toward higher energy observed in the condensed phase can be attributed to the effect of the substrate on the DEA mechanism. On one hand, the TMA lies at lower energy due to the polarizability of the molecular solid film. On the other hand, only anions having sufficient kinetic energy to overcome the attractive barrier induced by this polarizability at the surface of the solid contribute to the desorption yield.[30,62,63] This latter effect increases the energy of the DEA peak seen in yield functions. The resulting peak energy depends on a number of parameters such as mass of the anion, dissociation energy, film thickness, film polarizability, and orientation of the fragmented bond.[62,63] Furthermore, single or multiple electron energy losses to phonon and vibrational excitation within the solid also contribute to an upward shift of the energy position of the resonance.[61] Single or multiple energy losses are likely to occur with our films of approximately 10 ML thickness. The shifting of resonance peaks toward higher energies for anion production in the condensed phase, with respect to the gas phase, has been observed previously.[48,52,63] Also, as mentioned earlier in this section, in the case of amino acids it may be more difficult to compare data between gas and condensed phases, since the structure of these molecules and therefore their electronic configurations are expected to change from "neutral" or zwitterions.

Within the investigated incident electron energy range, the O^- fragment may be produced via either single or double bond breakage of the amino acid twin ion, $NH_3^+-...-COO^-$. In the case of single bond scission, the thermodynamic threshold, $E_{thr}(O^-)$, for O^- formation corresponds to the $C-O^-$ bond dissociation energy (BDE), that is, 2.15 eV.[64] For the double C=O bond breakage, $E_{thr}(O^-)$ can be expressed as the difference between the electron affinity of oxygen (i.e., 1.45 eV[35]) and the double-bonded carbon−oxygen BDE (i.e., 7.5 eV[64]). It is

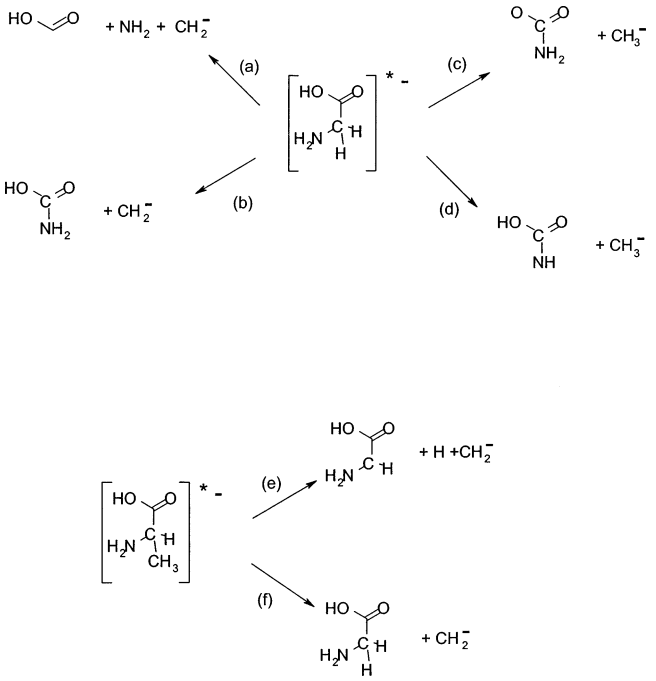

Figure 7. Possible dissociation pathways for (a,b) CH_2^- and (c,d) CH_3^- production after low-energy electron attachment to glycine. Reactions e and f represent possible pathways for CH_2^- fragmentation from alanine. Via reaction f, alanine is transformed into glycine.

then found $E_{thr}(O^-) = 6.05$ eV. The experimental threshold of detection of O^- species from electron impact onto films of glycine, alanine, and cysteine is measured to be approximately 4.0 eV (Figures 4d, 5c, and 6a, respectively), suggesting that at least near threshold O^- arises from the negatively charged oxygen atom of the zwitterion, that is, single bond rupture. Such a dissociation can be induced by direct scattering and may explain the absence of strong resonance peaks in the O^- yield function of glycine. The zwitterion configuration may not be necessary to produce O^- above ~6 eV. In fact, O^- is observed even below 6 eV from many gas-phase oxygen-containing compounds where the zwitterionic configuration is not present.[47] Thus, at higher energies, O^- anions could also arise from the C═O bond rupture, most likely via the capture of excess electron into a π^* orbital. Afterward, the extra electron may flow preferentially toward the oxygen atom, concomitantly stretch of the C═O bond, to form the desorbing O^- ion. Production of O^- induced by dissociation of the C═O bond has been reported earlier in DEA to gas-phase CO_2[65] and in electrons stimulated desorption of O^- from films of CO_2.[62,66]

Around 7.5 eV, a sharp peak is also observed in the CH^-, CH_2^-, and CH_3^- yield functions of glycine films and in the CH_2^- and CH_3^- yield functions of alanine films. Formation of CH_3^- and CH_2^- from alanine can simply be explained by unimolecular dissociation of the C−CH_3 and CH−CH_2 bonds with electron stabilization on the CH_3 and CH_2 radicals, respectively. Desorption of CH^- and CH_2^- from glycine requires a more complex reaction involving the scission of two bonds, as shown in Figure 7a,b for the case of CH_2^- formation. Moreover, the production of CH_3^- induced by the fragmentation of Gly is unexpected here, since no methyl group is present within the structure of glycine molecule. Therefore, this negative fragment may arise via (1) capture of hydrogen atom induced by collision of a CH_2^- anion or (2) a concerted reaction with atom "scrambling" or both.[67−70] The latter mechanism requires at least the shift of a hydrogen atom and, thus, involves more substantial change of nuclear coordinates. This may occur when the lifetime of the transient parent anion is sufficiently long to sustain deformation of molecular orbitals and rearrangement of the nuclei. However, the molecular dissociation must proceed before auto-ionization takes place. Concerted reactions for molecular fragmentation induced by electron impact with the displacement of a hydrogen atom have been reported below 10 eV for DEA to ethylene carbonate.[68] In our case, hydrogen atom capture by the CH_2^- anion is likely to have a minor contribution to methyl anion production; otherwise, the CH_3^- signal would be found to be smaller than that of CH_2^-. If we take into account the probability for CH_2^- to collide and react with the target to produce CH_3^- and the probability of the latter to desorb, the CH_3^- signal should be considerably smaller than the CH_2^- signal. In contrast, the signal of methyl anion is found to be 1 order of magnitude larger than that of CH_2^-. These results strongly suggest that TMA fragmentation operates via competitive dissociative pathways as exemplified in Figure 7 for the case of Gly. Along the repulsive potential energy surface of $(Gly)^{*-}$, the transient $(Gly)^-$ anion may decay along the $(NH_3^+-CH_2-CO^-)-O^-$ coordinate, up to the crossing point where different dissociative channels may become accessible.[70] In the case of a concerted reaction, displacement of a hydrogen atom, for instance, would lead to the formation of methyl anion as shown by reactions c and d in Figure 7. According to these latter, during the formation of the transient glycine anion, cleavage of the C−C and the C−N bond, as well as the formation of C−$N(H_2)$ or C−N(H) bond, should also occur. For example, the thermodynamic threshold, $E_{thr}(CH_3^-)$, for reaction 7d, can be expressed by $EA(CH_3) - (D(C-C) + D(N-H)) + D(C-H)$; $EA(CH_3)$ represents the electron affinity of CH_3, and $D(X-Y)$ represents the X−Y dissociation bond energy. Using the values of $EA(CH_3) = 0.08$ eV[35] and $D(C-C) = 3.5$ eV, $D(N-H) = 4.0$ eV, and $D(C-H) = 4.3$ eV[64] found in the literature, we then estimate $E_{thr}(CH_3^-)$ to be 3.2 eV. This estimate can be compared to 3.8 eV found experimentally for CH_3^- anion production threshold. This type of complex molecular fragmentation has been reported from UV irradiation of alanine; in particular, it has been shown via electron paramagnetic resonance (EPR) that the $CH_3-CH-OOH$ radical is formed when $NH_2-CH_3-CH-COOH$ is irradiated with UV photons.[71]

More surprisingly, neither CN^- nor CH^- were observed in anion desorption from condensed Ala with our detection limit. It should be noted that CH^- anion signal is also absent from the electron stimulated desorption yield of dimethyl disulfide[19] and thymine[18] where a methyl group is located at one end of the molecule.

Other structures in the CH_2^- and CH_3^- yield functions of glycine and alanine cannot easily be correlated. The peaks at 10.2 and 9.6 eV in the CH_2^- and CH_3^- yield functions of alanine films could arise from the additional electron of the TMA being localized close to the methyl moiety. These anion fragments were also reported at the same resonance energies in the electron stimulated desorption yield functions of C_2H_6 films.[72] The CH_2^- anion desorbed by electron impact on films of thymine, which structure also has a methyl group,[18] was reported at around 10.7 eV. Production of CH_2^- from the dissociation of an alanine transient anion may operate via the simplest reaction pathways represented in Figure 7, reactions e and f, respectively. The last dissociation mechanism produces additionally to CH_2^-, neutral glycine, whereas the second pathway generates hydrogen and glycyl radicals. The long-lived glycyl radical has been observed from X- and γ-irradiation of the glycine crystal.[73,74] Thermodynamic thresholds for reactions 7e and 7f are here estimated

to be 7.2−7.6 and 2.9−3.3 eV, respectively.[35,64] These values can be compared to ~5 eV found experimentally in the present work (Figure 5a), suggesting that at very low energies, alteration of alanine induced by LEEs generates glycine.

Although the CH_2 group exists within the structure of cysteine, we are not able to detect any signal of $CH_{(n=1,2,3)}^-$ anions generated from 1 to 40 eV electron bombardment of Cys films. However, we detect the higher mass negative fragments S^- and SH^-, in addition to H^-, O^-, OH^-, and CN^-. The formation of SH^- probably occurs via only a single S−C bond rupture, leaving the molecule in an alanyl radical configuration:

$$(NH_3^+-CHR'-COO^-)^{*-} \rightarrow SH^- + (NH_3^+-CHR''-COO^-)$$

where the radical R′ represents CH_2SH and R″, $CH_2^{\bullet}$. During the lifetime of the transient cysteine anion, S^- is likely to be generated via the following simplest pathway requiring a reorganization of the atoms:

$$(NH_3^+-CHR'-COO^-)^{*-} \rightarrow S^- + (NH_3^+-CHR'''-COO^-)$$

or

$$(NH_3^+-CHR'-COO^-)^{*-} \rightarrow S^- + (NH_3^+-CHR'''-COO^-) + H^{\bullet}$$

where R‴ stands for CH_3. The hydrogen atom at the sulfur site is transferred to the CH_2 site to form a methyl moiety, concomitantly to the production of the sulfur anion. This reaction shows that under LEE impact, cysteine can be transformed into alanine. On the other hand, the generation of S^- could be induced by two bond ruptures (i.e., S−C and S−H) giving birth to alanyl and hydrogen radicals. Both fragmentation pathways only differ by hydrogen recombination to the R″ group that stabilizes the radical group by approximately 4.4 eV (i.e., D(C−H)).[64] The yield function of S^- exhibits a peak at 4.6 eV, which may arise from the excitation of the σ^* (C−S) orbital. The location of this peak is found to be in agreement with that observed at 5.9 eV from low-energy electron impact on gas-phase cysteine experiments.[75] The red shift can be attributed to the effects of the solid on DEA and ion desorption.[30] This suggestion is inspired by the results of Dezarnaud et al. on LEE transmission and sulfur K-shell photoabsorption spectroscopies of the CH_3SH and CH_3-CH_2SH molecules, which can model the $-CH_2SH$ group of cysteine. They have reported a very broad structure ($\Delta E = 2.5$ eV) located at 2.9 eV.[75] The effect of the substrate upon heavy anion desorption (i.e., the cut off for the desorption of large mass fragments) may explain the shift in the resonant energy observed presently. The peak observed at 22 eV in both the yield functions of S^- and SH^- can be attributed to DEA or decay of the transitory anion into DD continuum or both, possibly with a small contribution from multiple events, as discussed previously for H^- desorption.

Sensitivity of Amino Acids to Low-Energy Electrons. It has been previously shown that LEEs are able to damage nucleic acids by fragmenting their basic components.[15−20] We have averaged over the 1−40 eV range the amount of desorbed anion fragments per incident electron for each aliphatic amino acid. Since absolute yields are not available from the present experiment and an estimate of the damage produced by LEEs from these yields requires multiple scattering calculations[76] or Monte Carlo simulations,[77] we cannot make comparisons with other types of radiobiological damage. It is possible, however, to make relative comparisons with results obtained under similar conditions. It is found that 0.2 CH^-, 0.3 CH_2^-, 2.3 CH_3^-, 0.05 O^-, 0.1 OH^-, and 2.5 $CN^- \times 10^{-10}$ ion/incident electrons are produced from glycine fragmentation, respectively. For the (CH_2^-, CH_3^-, O^-, and OH^-) and (O^-, OH^-, CN^-, S^-, and SH^-) negative species generated from fragmentation of alanine and cysteine, it is found that (1.8, 5.0, 1.3, and 1.0) $\times 10^{-10}$ and (2.0, 0.5, 0.5, 180, and 180) $\times 10^{-10}$ ion/incident electrons are desorbed, respectively. The average of total "heavy" ions desorbed from the fragmentation of glycine, alanine, and cysteine is estimated to be (5.5, 9.0, and 363) $\times 10^{-10}$ ion/incident electrons. Considering that cysteine also produces the highest H^- yield, it is clearly seen that according to these anion yields cysteine is the most sensitive of the investigated amino acids to LEE attack. Furthermore, the contribution to the total production of "heavy" ions, that is, (O^-, OH^-, and CN^-) and (CH_2^- and CH_3^- or S^- and SH^-) negative fragments, can arise from mainly two contributions: the first most likely is provided by the "twin-ion" group ($NH_3^+-...-COO^-$) and the second by the radical (R). For alanine, the two contributions are found to be (2.3 and 6.8) $\times 10^{-10}$ ion/incident electrons, respectively; for cysteine, (3.0 and 360) $\times 10^{-10}$ ion/incident electrons, respectively. This finding indicates that the zwitterionic group of aliphatic amino acids is likely to be less sensitive to LEEs than the neutral radical group. Moreover, this sensitivity may also depend partly on the length of the aliphatic amino acid and on the nature of the end group of R. In fact, the presence of the sulfur group enhances the production of fragments by 2 orders of magnitude. Such a strong enhancement has been previously reported from the investigation of electron stimulated desorption from films of dimethyl disulfide and acetamide.[19]

V. Conclusion

This work represents the third of a series of investigations on the effect of low-energy (<40 eV) electrons on protein constituents. We have shown that slow electrons dissociate the aliphatic amino acids glycine, alanine, and cysteine and produce H^- anions as the most intense fragment via simple bond cleavage. More complex molecular fragmentation also occurs to form various anionic species such as CH^-, CH_2^-, CH_3^-, O^-, OH^-, CN^-, S^-, and SH^-. Interestingly at certain energies, electrons can transform alanine to glycine and glycine and cysteine to alanyl and alanine. These alterations may modify the functionality of peptides and proteins. Below 15 eV, dissociation leading to anion production is mainly controlled by dissociative electron attachment. At higher energy, although nonresonant dipolar dissociation contributes to fragmentation of the molecule, it nevertheless competes with resonant processes: dissociative electron attachment or decay of the transient molecular anion into the dipolar dissociation continuum or both. This is seen from the structure located at around 20 eV in the H^- yield functions. Depending on the nature of the target molecule, the formation of transient molecular anions can arise from the trapping of the incoming electron on the zwitterionic glycine-like $NH_3^+-R-COO^-$ group or on the end of the radical, R, or both. For example, electron induced fragmentation of cysteine produces (O^-, OH^-, and CN^-) and (S^- and SH^-), which arise from the zwitterionic and R group, respectively. No CH^- or CH_2^- anions were detected for cysteine although R represents $-CH_2-SH$.

Acknowledgment. This work was supported by the Canadian Institutes of Health Research (CIHR).

References and Notes

(1) Wheldon, T. E. *Phys. Med. Biol.* **2000**, *45*, R77−R95.

(2) Lecas, C. In *Irradiation proposed to treat food*, Food & Drug *Administration*; FDA Consumer; FAO/IAEA/WHO International Conference on ensuring the safety and quality of food through radiationprocessing, Antalya, Turkey, 19−22 Oct. 1999; p 11−13 (194).

(3) Epstein, S. S.; Hauter, W. *Int. J. Health Serv.* **2001**, *31*, 187−192.

(4) Thayer, D. W.; Josephson, E. S.; Brynjofsson, A.; Giddings, G. G. *Counc. Agric. Sci. Technol. Issue Pap.* **1996**, *7*, 1−10.

(5) Gundestrup, M.; Storm, H. H. *The Lancet* **1999**, *354*, 2029.

(6) *ICRU Report.* International Commission on Radiation Units and Measurements: Washington, DC, 1979; Vol. 31.

(7) Pimblott, S. M.; Mozumder, A. *J. Phys. Chem.* **1991**, *95*, 7291−7300.

(8) Cobut, V.; Fongillo, Y.; Patau, J. P.; Goulet, T.; Fraser, M. J.; Jay-Gerin, J. P. *Radiat. Phys. Chem.* **1998**, *51*, 229−243.

(9) Ward, J. F. *Radiat. Res.* **1085**, *104*, S-103−S-111 and references therein.

(10) Pogozelski, W. K.; Tullius, T. D. *Chem. Rev.* **1998**, *98*, 1089−1107.

(11) Stadman, E. R. *Annu. Rev. Biochem.* **1993**, *62*, 797−821 and references therein.

(12) Ishizaki, S.; Ogasawara, M.; Tanaka, M.; Tagushi, T. *Fish. Sci.* **1994**, *60*, 603−606.

(13) Folkard, M.; Prise, K. M.; Vojonovic, V.; Davis, S.; Roper, M. J.; Michael, B. D. *Int. J. Radiat. Biol.* **1993**, *64*, 651−658.

(14) Boudaïffa, B.; Cloutier, P.; Hunting, D.; Huels, M. A.; Sanche, L. *Science* **2000**, *287*, 1658−1660.

(15) Abdoul-Carime, H.; Dugal, P. C.; Sanche, L. *Radiat. Res.* **2000**, *153*, 23−28.

(16) Simpson, W. C.; Orlando, T. M.; Parenteau, L.; Nagesha, K.; Sanche, L. *J. Chem. Phys.* **1998**, *108*, 5027−5034.

(17) Antic, D.; Parenteau, L.; Lepage, M.; Sanche, L. *J. Phys. Chem. B* 1999, *103*, 6611−6619.

(18) Abdoul-Carime, H.; Cloutier, P.; Sanche, L. *Radiat. Res.* **2001**, *155*, 625−633.

(19) Abdoul-Carime, H.; Cecchini, S.; Sanche, L. *Radiat. Res.* **2002**, *158*, 23−31.

(20) Abdoul-Carime, H.; Sanche, L. *Radiat. Res.* **2003**, *160*, 86−94.

(21) Hervé du Penhoat, M. A.; Huels, M. A.; Cloutier, P.; Jay-Gerin, J.-P.; Sanche, L. *J. Chem. Phys.* **2001**, *114*, 5755−5764.

(22) Gaubert, C.; Baudoing, R.; Gauthier, Y.; Michaud, M.; Sanche, L. *Appl. Surf. Sci.* **1986**, *25*, 195−202.

(23) Leclerc, G.; Goulet, T.; Jay-Gerin, J.-P.; Sanche, L. *J. Chem. Phys.* **1987**, *91*, 4999−5001.

(24) Langlois, R.; Ali, H.; Brasseur, N.; Wagner, R.; van Lier, J. E. *Photochem. Photobiol* **1986**, *44*, 117.

(25) Sanche, L. *J. Chem. Phys.* **1979**, *71*, 4860−4882.

(26) Rowntree, P.; Parenteau, L.; Sanche, L. *J. Phys. Chem.* **1991**, *95*, 4902−4908.

(27) Nyberg, M.; Hasselström, J.; Karis, O.; Wassdahl, N.; Weinelt, M.; Nilsson, A.; Pettersson, L. G. M. *J. Chem. Phys.* **2000**, *112*, 5420−5427.

(28) Patthey, L. Ph.D. Thesis, Université de Lausanne, Switzerland, 1995.

(29) *Handbook of Chemistry Physics*, 73th ed.; Lide, D. R., Ed.; CRC Press: Boca Raton, FL, 1992−1993.

(30) Sambe, H.; Ramaker, D. E.; Parenteau, L.; Sanche, L. *Phys. Rev. Lett.* **1987**, *59*, 236−239.

(31) Gohlke, S.; Rosa, S. A.; Illenberger, E.; Bruning, F.; Huels, M. A. *J. Chem. Phys.* **2002**, *116*, 10164−10170.

(32) Antic, D.; Parenteau, L.; Lepage, M.; Sanche, L. *J. Phys. Chem. B* **1999**, *103*, 6611−6619.

(33) Budzikiewicz, H. *Angew. Chem., Int. Ed. Engl.* **1981**, *20*, 624−637.

(34) Huels, M. A.; Parenteau. L.; Sanche, L. *Chem. Phys. Lett.* **1997**, *279*, 223−229.

(35) Janousek, B. K.; Brauman, J. I. In *Gas-Phase Ion Chemistry*; Bowers, M. T., Ed.; Academic Press: New York, 1979.

(36) Junk, G.; Svec, H. *J. Am. Chem. Soc.* **1963**, *85*, 839.

(37) Gaffney, J. S.; Pierce, R. C.; Friedman, L. *J. Am. Chem. Soc.* **1977**, *99*, 4293.

(38) Grenie, Y.; Lassegues, J.-C.; Garrigou-Lagrange, C. *J. Chem. Phys.* **1970**, *53*, 2980.

(39) Reva, I. D.; Plokhotnichenko, A. M.; Stepanian, S. G.; Ivanov, A.; Radchenko, E. D.; Sheina, G. G.; Blagoi, Y. P.; *Chem. Phys. Lett.* **1995**, *232*, 141−148; Erratum, *Chem. Phys. Lett.* **1995**, *235*, 617.

(40) Huckel, W. In *Theoretical Principle of Organic Chemistry*; Elsevier: New York, 1968; Vol. II, pp 150−157.

(41) Jönsson, P.-G.; Kvick, Å. *Acta Crystallogr. B* **1972**, *28*, 1827.

(42) Uvdal, K.; Bodö, P.; Liedberg, B. *J. Colloid Interface Sci.* **1992**, *149*, 162−173.

(43) Leggett, G. J.; Davies, M. C.; Jackson, D. E.; Tendle, S. J. B. r. *J. Phys. Chem.* **1993**, *97*, 5348−5344.

(44) Destro, R.; Roversi, P.; Barzhaghi, M.; Marsh, R. E. *J. Phys. Chem. A* **2000**, *104*, 1047−1054.

(45) Bowen, K. H. Private communication. Bowen, K. H. At the Euresco Conference on "Molecules of Biological Interest in the Gas Phase", Euresco Conference on Experimental Tools and Quantum Chemistry, Les Houches, France, 2000.

(46) Fernandez-Ramos, A.; Smedarchina, Z.; Siebrand, W.; Zgierski, M. Z. *J. Chem. Phys.* **2000**, *113*, 9714−9721.

(47) Christophorou, L. G. *Electron−Molecule Interactions and their Applications*; Academic Press Inc.: New York, 1984; Vol. 1.

(48) Sanche, L. In *Excess Electrons in Dielectric Media*; Ferradini, C., Jay-Gerin, J.-P., Eds.; CRC Press: Boca Raton, FL, 1991.

(49) Ingòlfson, O.; Weik, F.; Illenberger, E. *Int. J. Mass Spectrom. Ion Processes* **1996**, *155*, 1−68.

(50) Dugal, P. C.; Huels, M. A.; Sanche, L. *Radiat. Res.* **1999**, *151*, 325−333.

(51) Huels, M. A.; Hahndorf, I.; Illenberger, E.; Sanche, L. *J. Chem. Phys.* **1998**, *108*, 1309−1312.

(52) Sanche, L. *Scanning Microsc.* **1995**, *9*, 619−656.

(53) Sanche, L. *Radiat. Chem.* **1993**, *40*, 28−39.

(54) Schulz, G. J. *Rev. Mod. Phys.* **1973**, *45*, 423−486.

(55) Sanche, L.; Schulz, G. J. *Phys. Rev. A* **1972**, *6*, 69−86.

(56) Gutowski, M.; Skurski, P.; Simons, J. *J. Am. Chem. Soc.* **2000**, *122*, 10159−10162.

(57) Aflatooni, K.; Hitt, B.; Gallup, G. A.; Burrow, P. D. *J. Chem. Phys.* **2002**, *16* 6489−6492.

(58) Powis, I. *J. Chem. Phys.* **2000**, *104*, 878−882. Klasine, L. *J. Electron Spectrosc. Relat. Phenom.* **1976**, *8*, 161−164.

(59) Neville, J. J.; Zheng, Y.; Brion, C. E. *J. Am. Chem. Soc.* **1996**, *118* 10533−10544.

(60) Antic, D.; Parenteau, L.; Sanche, L. *J. Phys. Chem. B* **2000**, *104*, 4711−4716.

(61) Azria, R.; Parenteau. L.; Sanche, L. *J. Chem. Phys.* **1987**, *87*, 2292−2296.

(62) Sanche, L. *Surf. Sci.* **2000**, *451*, 82−90.

(63) Huels, M. A.; Parenteau, L.; Sanche, L. *J. Chem. Phys.* **1994**, *100*, 3940−3956.

(64) Lowry, T. H.; Richardson, K. S. In *Mechanism and theory in organic chemistry*, 3rd ed.; Harper Collins Publisher: Toronto, Ont, 1987.

(65) Orient, O. J.; Srivastava, S. K. *Chem. Phys. Lett.* **1983**, *96*, 681−684.

(66) Huels, M. A.; Bass, A. D.; Ayotte, P.; Sanche, L. *Chem. Phys. Lett.* **1995**, *245*, 387−392.

(67) Pariat, Y.; Allan, M. *Int. J. Mass Spectrom. Ion Processes* **1991**, *103*, 181−192.

(68) Jacobsen, S.; Jensen, H.; Pedersen, S. U.; Daasbjerg, K. *J. Phys. Chem. A* **1999**, *103*, 4141−4143.

(69) Stepanovic, M.; Pariat, Y.; Allan, M. *J. Chem. Phys.* **1999**, *110*, 11376−11382.

(70) Abdoul-Carime, H.; Huels, M. A.; Brüning, F.; Illenberger, E.; Sanche, L. *J. Chem. Phys.* **2000**, *113*, 2517−2521.

(71) Cabral-P, A.; Urena-Nunez, F.; Jimenez-Dominguez, H. *J. Chem. Phys.* **1994**, *101*, 1967−1974. Miayagwa, I.; Gordy, G. *J. Chem. Phys.* **1960**, *32*, 255.

(72) Rowntree, P.; Parenteau, L.; Sanche, L. *J. Phys. Chem.* **1991**, *95*, 4090−4909.

(73) Brustolon, M.; Chis, V.; Maniero, A. L.; Brunel, J.-C. *J. Chem. Phys.* **1997**, *101*, 4887−4892.

(74) Box, H. C. *Radiation effects: ESR and ENDOR analysis*; Academic Press: New York, 1977.

(75) Dezarnaud, C.; Tronc, M.; Modelli, A. *Chem. Phys.* **1991**, *156*, 129−138.

(76) Ishii, M. A.; Kimura, M.; Inokuti, M. *Phys. Rev. A* **1990**, *42*, 6486−6496.

(77) Meesungnoen, J.; Jay-Gerin, J.-P.; Filali-Mouhim, A.; Mankhetkorn, S. *Radiat. Res.* **2002**, *158*, 657−660.